10-Gb/s BPSK link using Silicon Microring Resonators for Modulation and Demodulation

Qi Li[1*], Yang Liu[2*], Kishore Padmaraju[1], Ran Ding[2], Dylan F. Logan[3,4], Jason J. Ackert[3], Andrew P. Knights[3], Tom Baehr-Jones[2,7], Michael Hochberg[2,5,6], and Keren Bergman[1]

[1] Department of Electrical Engineering, Columbia University, 500 West 120th Street, New York, NY 10027, USA
[2] Department of Electrical and Computer Engineering, University of Delaware, Newark, DE 19716, USA
[3] Department of Engineering Physics, McMaster University, 1280 Main Street West, Hamilton, ON, Canada
[4] Currently with Ranovus Inc., Ottawa, ON, Canada
*[5] Institute of Microelectronics, A*STAR (Agency for Science, Technology and Research), 11 Science Park Road, Singapore Science Park II, Singapore 117685, Singapore*
[6] Department of Electrical & Computer Engineering, National University of Singapore, Singapore 117576, Singapore
[7] EastWest Photonics PTE LTD, 261 Waterloo Street #02-24, Waterloo Centre, Singapore 180261, Singapore
**Equal contribution. Author email address: ql2163@columbia.edu; phyliuyang@gmail.com.*

Abstract: We demonstrate the first binary-phase-shift-keying (BPSK) link based on silicon microring resonators, with an operational bit-rate at 10 Gb/s. Bit-error-rate measurements and eye diagrams are used to compare the link's performance with conventional BPSK modulation and demodulation techniques.

OCIS codes: (060.5060) Phase modulation; (230.4110) Modulators; (230.3120) Integrated optics devices.

1. Introduction

In recent years silicon photonics has gained a considerable amount of interest because it has the potential to offer compact, energy-efficient and cost-effective optical components, leveraging the complementary metal–oxide–semiconductor (CMOS) fabrication process. It has been proposed in a number of applications such as on-chip optical interconnect, nonlinear signal processing, optical access networks as well as next-generation computing systems [1-6], offering a potentially disruptive technology solution. For instance, combining its low-cost nature with the high volume market in the access network, silicon photonics could expedite fiber-to-the-home (FTTH) deployment and satisfy the increasing user bandwidth demand.

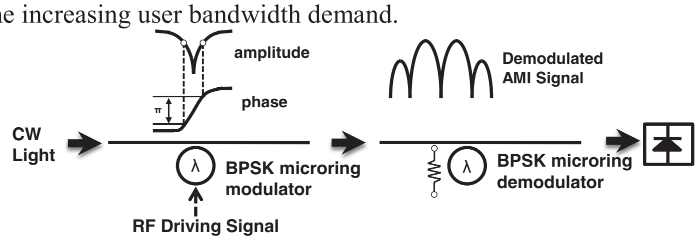

Fig. 1. Microring based BPSK link.

Compared with on-off-keying (OOK) format, BPSK has a higher tolerance to nonlinear degradation and provides 3-dB receiver sensitivity improvement with balanced detection. BPSK is usually generated using either a phase modulator or Mach-Zehnder modulator (MZM) and demodulated using a delay-line interferometer (DLI). Recently, microrings are gaining increasing attention in phase-modulated optical transmission systems. Microring-based BPSK modulation and demodulation are first proposed in [7]. A great advantage of microring-based BPSK is the easier application of wavelength division multiplexing (WDM) than alternative schemes. Microrings can be cascaded for WDM modulation in the transmitting side and for simultaneous WDM demultiplexing and BPSK demodulation in the receiving end, which can be realized in a very compact, power efficient and low-cost way. Our previous work have shown microring-based BPSK modulation and demonstrated its error-free transmission up to 80 km and resilience to dispersion at 5 Gb/s [8]. BPSK demodulation using silicon microring was demonstrated in [9]. In addition to BPSK, other microring-based advanced modulation formats, such as quadrature phase-shift-keying (QPSK), are demonstrated recently [10]. In this work we demonstrated for the first time, a microring-based BPSK link (Fig. 1) at 10 Gb/s, and compare its performance with conventional modulation and demodulation techniques using eye diagrams and bit-error-rate measurements.

2. Devices and experiment

The depletion-mode microring modulator (Fig. 2a), is fabricated via the shuttle service OpSIS [11] at the Institute of Microelectronics (IME). The microring modulator has a radius of 8um. It's formed by slab waveguide with 500nm width, 220nm height and 90nm slab height. The pn junction has a doping density of $2\times10^{18}/cm^3$ on the p side, and $3\times10^{18}/cm^3$ on the n side. The junction line has a 50nm offset from the center of the waveguide in order to optimize the modulation efficiency. For BPSK signal generation, the microring need to be overcoupled (i.e., waveguide-ring coupling coefficient > microring loss) so that when the microring resonance is shifted, at certain wavelength there will be π phase shift and the same optical power in each bit duration. To confirm the overcoupling condition, transmission spectrum of the microring modulator is recorded at different bias voltage (Fig 2b). It is obvious from the plots that when larger reverse bias is applied, the resonance peak of the microring experience a red shift, associated with a decreased extinction ratio, indicating the overcoupling condition is satisfied [8]. Q factor of the microring is measured to be ~4300, and the tunability of the microring is ~ 28pm/V.

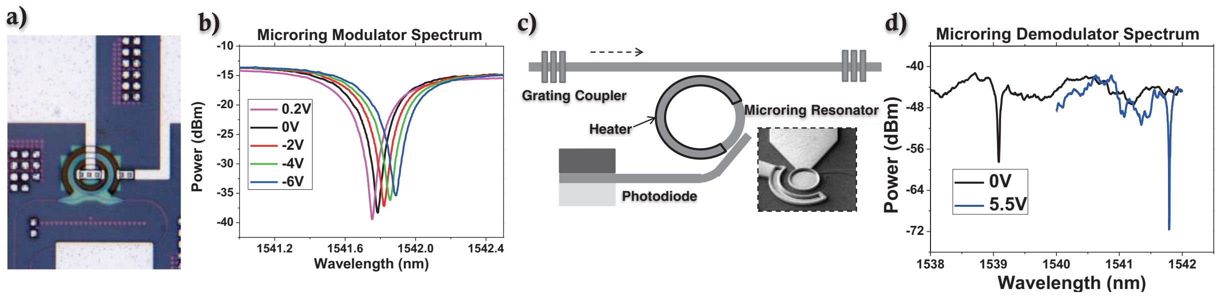

Fig. 2. a) Microring modulator image. b) Wavelength scans of the microring modulator at varying bias voltages. c) The microring demodulator with integrated heater and drop port photodetector (not to scale). Inset: SEM image of fully processed device. d) Microring demodulator spectrum at varying heater voltages.

The microring demodulator (Fig. 2c) is 15 µm in radius, and has a thin film heater directly above it. The waveguides have dimensions of 500 nm × 220 nm (width × height), and are etched to a depth of 170 nm. A defect-enhanced silicon photodiode is positioned at the microring drop port, however it is for optical power monitoring purpose [12] and cannot be used for high-speed signal detection. The microring demodulator has a Q factor of ~22,000 (0.07nm 3dB passband). For BPSK demodulation the microring through port acts as a notch filter to produce the alternate-mark inversion (AMI) signal and the drop port acts a band-pass filter to produce the duobinary signal [7]. Since we had no access to the drop port, only the demodulated AMI signal was recorded.

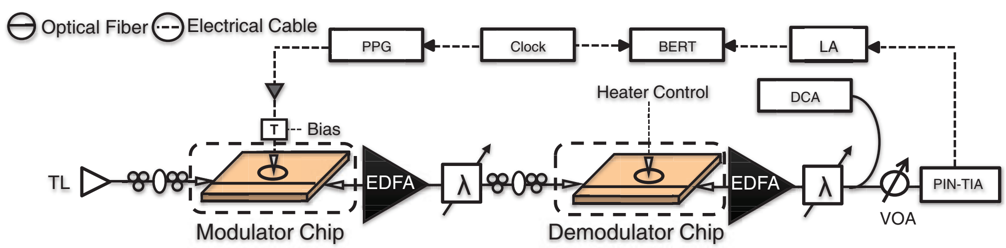

Fig. 3. Experimental Setup of microring modulated/demodulated BPSK.

In our experimental setup (Fig 3), a pulsed-pattern generator (PPG) was used to generate 10-Gb/s non-return-to-zero (NRZ) 2^{31}-1 pseudo-random-bit-sequence pattern (PRBS) RF signal. The signal was amplified to 3.3 V_{pp} and biased at 2.7 V to drive the microring modulator with a high-speed RF probe. A CW tunable laser (TL) at a wavelength of 1541.7 nm was set to TE polarization before being launched onto the modulator chip. The microring-modulated BPSK signal egressing from the chip was amplified with an erbium-doped fiber amplifier (EDFA), filtered (λ), and set to TE polarization before being launched onto the second chip for demodulation. The integrated heater voltage was set to 5.42 V, ensuring that the resonance of the microring demodulator aligns with the modulator wavelength. After the second chip, the demodulated signal passed through another EDFA, a filter and a variable optical attenuator (VOA), before being received on a PIN-TIA photodetector followed by a limiting amplifier (LA) and fed into a bit-error-rate tester (BERT) for BER measurements. The amplifiers may be eliminated in future integrated version where excessive coupling loss could be avoided. A digital communications analyzer (DCA) was used to record eye diagrams throughout the experiment. In order to compare the microring modulated/demodulated BPSK with conventional approach, MZM and DLI were used to replace the modulator and demodulator chip respectively, and a back-to-back case was done using only MZM and DLI.

Figure 4 shows the experimental results. The microring modulator was first tested to generate 10-Gb/s OOK (Fig. 4a). The wavelength was then tuned in order for bit states to have equivalent amplitudes, thus generating a BPSK signal (Fig. 4b). Compared with MZM-generated BPSK, the microring modulator exhibits both frequency chirp and intensity dips [7]. The microring generated BPSK was first demodulated by a commercial DLI demodulator (Fig. 4c), which was tuned to match the BPSK wavelength. The BPSK signal was then demodulated by the microring through port by generating the AMI signal (Fig. 4d). Note for 10-Gb/s BPSK demodulation, the optimal Q for maximal eye-opening is ~22,000 [7], close to the microring we used. We also tried microrings with Q of ~5,000, however no successful BPSK demodulation was achieved. For comparison, a MZM generated BPSK signal was also demodulated by the microring (Fig. 4e). Finally the MZM generated BPSK was demodulated by the DLI demodulator (Fig. 4f) for the back-to-back measurement. For all the measurements, clean and open eyes were obtained. The eye diagram shape difference between MZM-generated and microring-generated BPSK is due to the amplitude carving of microring resonance [8]. Fig. 4g shows the BER measurements collected for the different modulation-demodulation experiments. There is ~2 dB power penalty for microring-demodulated signal compared to the DLI demodulated signal, and higher penalty for microring-generated cases. Part of the power penalty is attributed to the ASE noise added by EDFA since the modulator and demodulator chips have large insertion loss compared with the commercial product. The varying slopes of the BER curves were due to a combination of the modulation chirp and microring filtering effect. However, even for the all-microring-based case, the obtained BER is below the forward error correction (FEC) limit, which validates the application of microring-based BPSK link for practical usage.

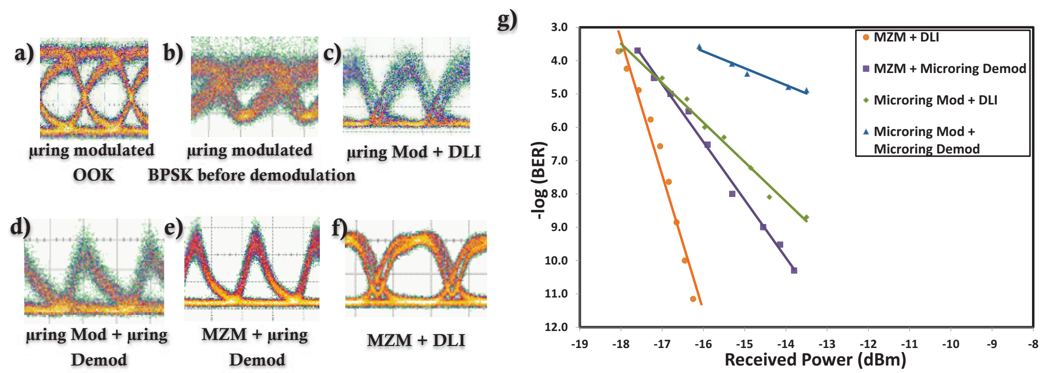

Fig. 4. a) Microring modulated OOK. b) Microring modulated BPSK before demodulation. c) Microring modulated BPSK demodulated by DLI. d) Microring modulated BPSK demodulated by microring demodulator. e) MZM modulated BPSK demodulated by microring. f) MZM modulated BPSK demodulated by DLI. g) Measured BER curves for different modulation/demodulation experiments.

3. Conclusion

We have demonstrated the first microring modulated BPSK signal at 10 Gb/s, and the first all microring-based BPSK link. The obtained BER is below the FEC limit, validating the practical application of the demonstrated technique. Compared with the traditional MZM and DLI based approach, the microring-based devices have substantially smaller footprints and can be potentially cascaded into arrays utilizing WDM for high-capacity transceivers. Furthermore, combination of microring-based BPSK can be used to produce QPSK modulators and demodulators [13], which can be used to build next generation coherent transceivers under stringent cost and power requirements.

The authors gratefully acknowledge support from AFOSR STTR grants FA9550-12-C-0079 and FA9550–12-C-0038, as well as an NRF Fellowship NRF2012NRF-NRFF001-143. The authors also would like to thank Gernot Pomrenke, of AFOSR, for his support of the OpSIS effort, through both a PECASE award (FA9550-13-1-0027) and ongoing funding for OpSIS (FA9550-10-l-0439).

4. References

[1] J. Leuthold *et al*."Nonlinear silicon photonics." Nature Photonics 4.8 (2010): 535-544.
[2] C. Batten *et al*. "Building many-core processor-to-DRAM networks with monolithic CMOS silicon photonics." IEEE Micro 29.4 (2009): 8-21.
[3] A. Poon *et al*. "Cascaded microresonator-based matrix switch for silicon on-chip optical interconnection." Proceedings of the IEEE 97.7 (2009): 1216-1238.
[4] Q. Li *et al*. "105 nm Wavelength Conversion of 40-Gb/s DPSK in a Dispersion-Engineered Silicon Waveguide." CLEO 2013 CTu1G.1
[5] L. Xu *et al*. "Colorless optical network unit based on silicon photonic components for WDM PON." IEEE Pho. Tech. Letters. 24(16) 1372-1374 (2012).
[6] Q. Li *et al*. "Scaling Star-Coupler-Based Optical Networks for Avionics Applications," IEEE J. Opt. Commun. Netw5 (9) (2013).
[7] L. Zhang *et al*. "Microring-based modulation and demodulation of DPSK signal". Opt. Express 15(18), 11564-11569 (2007).
[8] K. Padmaraju *et al*. "Error-free transmission of microring-modulated BPSK." Opt. Express 20 (2012): 8681-8688.
[9] L. Xu *et al*. "Optical differential-phase-shift-keying demodulation using a silicon microring resonator." IEEE Pho. Tech. Letters, 21(5): 295-297.
[10] P. Dong *et al*. "Silicon Microring Modulators for Advanced Modulation Formats." OFC 2013.
[11] C. Galland *et al*. "Systems and Devices in a 30 GHz Silicon-on-insulator Platform," ECOC Mo.3.B.2 (2013).
[12] K. Padmaraju *et al*. "Microring Resonance Stabilization using Thermal Dithering," IEEE Optical Interconnects Conference 2013 TuC5.
[13] L. Zhang *et al*. "Monolithic modulator and demodulator of differential quadrature phase-shift keying signals based on silicon microrings." Optics letters 33.13 (2008): 1428-1430.